SPIE IT Com (Information Technology and Communication) 25-28 October 2004, Philadelphia, Pennsylvania, USA. Proc. SPIE Vol. 5597, p. 82-96, Nanophotonics for Communication: Materials and Devices; Michal F. Lipson, George Barbastathis, Achyut K. Dutta, Kiyoshi Asakawa; Eds., Oct. 2004

Photonic nanostructures for wavelength division multiplexing

Martina Gerken[*a], David A. B. Miller[b]
[a]Lichttechnisches Institut, Universität Karlsruhe (TH), Kaiserstraße 12, 76131 Karlsruhe, Germany;
[b]Edward L. Ginzton Laboratory, Stanford University, Stanford, CA, USA 94305

ABSTRACT

The high angular dispersion achieved with the photonic crystal superprism effect as well as dispersive non-periodic photonic nanostructures promise compact wavelength division multiplexing (WDM) devices. An important criterion for the usefulness of such WDM devices is the number of channels that a structure can multiplex or demultiplex. Here two different models are developed for calculating the possible number of channels for a given structure. The first model is based on the assumption that different wavelength channels should propagate in mutually exclusive propagation cones within the volume of the dispersive structure. We call these non-overlapping channels "volume modes." The second model assumes that it is sufficient to spatially separate the different wavelength channels on a single output surface, e.g., the plane of the detectors or output waveguides. Since they are only separated along one surface and not in the entire volume, we name these modes "surface modes." As an example it is shown that a dispersive 200-layer non-periodic thin-film stack can be used to multiplex or demultiplex approximately eight WDM channels. The achievable number of channels is not defined by the dispersion alone but by the product of dispersion and wavelength range over which this dispersion is achieved.

Keywords: photonic crystals, multilayer thin-film stacks, superprism, dispersion, wavelength division multiplexing

1. INTRODUCTION

High angular dispersion based on a rapid change of the group propagation angle with wavelength in a photonic crystal has been termed the "superprism effect" and has been observed experimentally in planar [1] and thin-film [2] one-dimensional, in two-dimensional [1, 3], and in three-dimensional [4] photonic crystals. We have demonstrated previously that not only periodic, but also non-periodic photonic nanostructures can be designed to exhibit high dispersion [5]. We focus on one-dimensional nanostructures, since these can be realized reliably and cost-effectively as multilayer thin-film stacks. We introduced four algorithms for designing thin-film stacks with high dispersion based on periodic structures using the "superprism effect" in one-dimensional photonic crystals, chirped structures, resonator structures, and numerically optimized non-periodic structures [5]. We experimentally demonstrated that is it possible to custom-engineer the dispersion properties to obtain, for example, a linear beam shifting as a function of wavelength [6] or a step-like beam shifting [7]. A step-like beam shifting with wavelength is particularly interesting for communications devices as it corresponds to flat-top passbands. Here we develop a model for predicting how many WDM channels can be multiplexed or demultiplexed using a given one-dimensional photonic nanostructure. We investigate the influence of the dispersion, the incidence angle, the input beam diameter, and the crosstalk requirements on the number of spatially separable channels. In contrast to previous results [8] we show that it is not necessary to use large beam diameters to separate the maximum number of WDM channels.

The spatially separable WDM channels are referred to as "modes" of the structure. First we need to define what is meant by a mode of the structure. As we are investigating structures with a continuous shift as a function of wavelength, all wavelengths can propagate through the structure. A mode is therefore not defined by the fact that it propagates through the structures whereas other modes do not. Hence this definition is unlike that of modes in a waveguide. A mode is also not defined by the fact that it can be physically distinguished from other modes. Since different wavelengths are associated with the different modes, they can always be distinguished.

[*] Tel.: +49-721-608-3981, Fax: +49-721-358149, Email: martina.gerken@lti.uni-karlsruhe.de

Our definition of a mode is related to the spatial extent of a channel without considering its wavelength. Rigorously, perhaps, our modes are beam forms that are spatially orthogonal. Beams that do not overlap at all are certainly spatially orthogonal and other orthogonal patterns might also be possible, e.g., as in the communication modes of [9]. Beams that mostly do not overlap can be considered approximately orthogonal, and do lead to the right overall counting of such modes as discussed in [9]. This definition is based on the idea that we want to use the dispersion of multilayer structures to spatially separate channels of different wavelengths, i.e. we want to measure the power of a demultiplexed channel without considering its wavelength. The question of the number of modes of a given stack is therefore equivalent to the question of how many separate channels can we demultiplex assuming wavelength-insensitive detectors.

Two possible types of spatial modes are considered as depicted in Fig. 1. “Volume modes” are defined as being modes that have mutually exclusive propagation cones within the volume of the stack as shown in Fig. 1(a). “Surface modes” may overlap within the volume of the stack, but are separated on the exit surface as seen in Fig. 1(b). For the case of surface modes the effect of multiple passes through the stack as shown in Fig. 1(c) is considered as well.

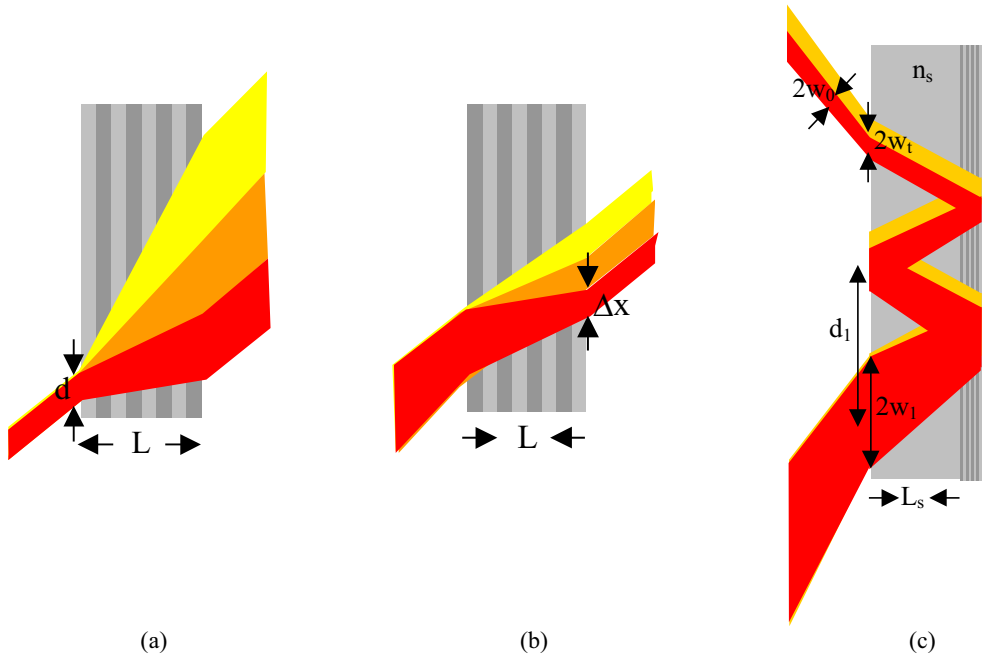

Fig. 1. (a) Volume modes. (b) Surface modes. (c) Surface modes including multiple bounces off the stack with the substrate as spacer. The multiplexed light is incident from the bottom left in each case.

This paper is structures as follows: In section 2 a method for approximating the number of volume modes as depicted in Fig. 1(a) is presented. In section 3 the approximate number of volume modes for a design with a linear change in the group propagation angle with wavelength is calculated and verified by a numerical simulation. In section 4 an equation for calculating the number of surface modes as shown in Fig. 1(b) is introduced. In section 5 this surface mode model is extended to include multiple bounces off a stack and Gaussian beam propagation through a spacer as illustrated in Fig. 1(c). Section 6 verifies the surface mode model by comparison to numerical simulation for the design with a linear change in the group propagation angle with wavelength. Finally, in section 7 it is shown that a design with a linear change in the beam shifting along the output surface with wavelength is advantageous as all modes have the same focal plane parallel to the output surface thus allowing the largest number of modes to be multiplexed with just a single focusing lens. The paper finishes with conclusions in section 8.

2. NUMBER OF VOLUME MODES

In this section we are going to consider the number of volume modes that can be separated by a structure. Here we do not consider what happens for multiple bounces and intermediate propagation through the substrate. We define volume

modes as modes that propagate in mutually exclusive propagation cones. For simplicity we will assume a device as shown in Fig. 1(a). Plane waves of different wavelengths propagate at different angles within the device. As shown in [7], a monochromatic beam of light can be decomposed into plane-wave components with different propagation directions. Thus, a beam of light consists of a range of propagation angles. In principle a beam has components at all angles, but many of these might have very small amplitudes and can thus be neglected. Here we consider the angular range to be delimited by those components whose intensity has dropped to $1/e^2$ from the center component. For less crosstalk between channels a wider angular range may be chosen, which only results in a scaling of the results given here.

Assuming the input beam of multiplexed wavelengths is focused on the front of the device and that the input diameter of the beam d is small compared to the width of the device L (see Fig. 1(a)), modes are non-overlapping in the volume and at the output if their angular ranges are non-overlapping within the structure. If, for example, the first mode has an angular content within the device of 10º to 20º and the next mode occupies the angular range from 20º to 30º, these modes will not overlap at the output and are thus separate modes. Following this definition of separable modes, the number of modes within a small frequency range $\Delta\omega$ is given by (1).

$$\Delta N_{\mathrm{mod}es}\left(\tilde{\theta},\tilde{\omega},\Delta\omega,\Delta\theta_{in}\right)=\frac{\theta_{group}\left(\tilde{\theta},\tilde{\omega}+\Delta\omega/2\right)-\theta_{group}\left(\tilde{\theta},\tilde{\omega}-\Delta\omega/2\right)}{\Delta\theta_{struc}\left(\tilde{\theta},\tilde{\omega},\Delta\theta_{in}\right)} \tag{1}$$

In this equation $\Delta\theta_{struc}$ is the angular range of a mode within the structure for a given angular range $\Delta\theta_{in}$ of the input beam in vacuum. θ is the incidence angle of the beam, θ_{group} is the group propagation angle in the stack, and ω is the frequency. The dispersion relation can be expressed either in terms of the incidence angle and the frequency $\left(\tilde{\theta},\tilde{\omega}\right)$ or in terms of the wavevector parallel to the layers β and the frequency $\left(\beta,\omega\right)$. In order to distinguish these two sets of variables we use the tilde for the first case. The variable transformation between $\left(\tilde{\theta},\tilde{\omega}\right)$ and $\left(\beta,\omega\right)$ is discussed in [10]. Defining the dispersion $Disp_\omega$ as shown in (2), the total number of modes between ω_1 and ω_2 is given by (3).

$$Disp_{\omega}\left(\tilde{\theta},\tilde{\omega}\right)=\frac{\partial\theta_{group}\left(\tilde{\theta},\tilde{\omega}\right)}{\partial\tilde{\omega}} \tag{2}$$

$$N_{\mathrm{mod}es}\left(\tilde{\theta},\omega_1,\omega_2,\Delta\theta_{in}\right)=1+\int_{\omega_1}^{\omega_2}\Delta N_{\mathrm{mod}es}\left(\tilde{\theta},\tilde{\omega},d\tilde{\omega},\Delta\theta_{in}\right)=1+\int_{\omega_1}^{\omega_2}\frac{Disp_{\omega}\left(\tilde{\theta},\tilde{\omega}\right)}{\Delta\theta_{struc}\left(\tilde{\theta},\tilde{\omega},\Delta\theta_{in}\right)}d\tilde{\omega} \tag{3}$$

Note there has to be one mode even without any dispersion, since one beam can always simply propagate through the structure. To evaluate this number of modes, we need to find an expression for $\Delta\theta_{struc}$. $\Delta\theta_{struc}$ can be estimated from $\Delta\theta_{in}$ using (4), where the difference is approximated by a differential.

$$\Delta\theta_{struc}\left(\tilde{\theta},\tilde{\omega},\Delta\theta_{in}\right)=\frac{\partial\theta_{group}\left(\tilde{\theta},\tilde{\omega}\right)}{\partial\tilde{\theta}}\Delta\theta_{in} \tag{4}$$

In order to relate $\Delta\theta_{struc}$ to the dispersion $Disp_\omega$, the group velocity angle θ_{group} is developed into a Taylor series [10]. This results in relationship (5) between the angular range $\Delta\theta_{struc}$ of a beam within a dispersive stack, the input angular range $\Delta\theta_{in}$, and the dispersion of the stack $Disp_\omega$.

$$\Delta\theta_{struc}\left(\tilde{\theta},\tilde{\omega},\Delta\theta_{in}\right)=\left(\frac{\cos\tilde{\theta}}{\sqrt{{n_{avg}}^2-\sin^2\tilde{\theta}}}+Disp_{\omega}\left(\tilde{\theta},\tilde{\omega}\right)\frac{\tilde{\omega}\cos\tilde{\theta}}{\sin\tilde{\theta}-c\dfrac{\partial\beta}{\partial\omega}}\right)\Delta\theta_{in} \tag{5}$$

Since $\partial\beta/\partial\omega$ is approximately constant with wavelength [10], the only rapidly varying term with wavelength in (5) is the dispersion $Disp_\omega$. Thus, the angular range of a mode $\Delta\theta_{struc}$ can be estimated as the input angular range $\Delta\theta_{in}$ multiplied by the sum of a constant term added to a term that is proportional to the dispersion. The validity of this approximation is limited to stacks that have a constant angular dispersion or to small input angular ranges as differences are replaced by differentials. Substituting expression (5) for $\Delta\theta_{struc}$ into (3), we obtain the number of volume modes within a given wavelength range as given in (6).

$$N_{modes}\left(\tilde{\theta},\omega_1,\omega_2,\Delta\theta_{in}\right)=1+\int_{\omega_1}^{\omega_2}\frac{1}{\left(\frac{\cos\tilde{\theta}}{Disp_\omega\left(\tilde{\theta},\tilde{\omega}\right)\sqrt{n_{avg}{}^2-\sin^2\tilde{\theta}}}+\frac{\tilde{\omega}\cos\tilde{\theta}}{\sin\tilde{\theta}-c\frac{\partial\beta}{\partial\omega}}\right)}\frac{1}{\Delta\theta_{in}}d\tilde{\omega} \qquad (6)$$

(6) reveals that the number of volume modes is inversely proportional to the input angular range. Thus, half the input angular range means double the number of modes, and double the input range half the number of modes. This result was verified in simulations presented in the following section.

The interesting part of (6) is the denominator of the first fraction. It can be seen that for small dispersions, $\cos\tilde{\theta}\Big/\left(Disp_\omega\left(\tilde{\theta},\tilde{\omega}\right)\sqrt{n_{avg}{}^2-\sin^2\tilde{\theta}}\right)$ dominates and the number of modes increases linearly with increasing dispersion. For large dispersion values on the other hand, $\tilde{\omega}\cos\tilde{\theta}\Big/\left(\sin\tilde{\theta}-c\frac{\partial\beta}{\partial\omega}\right)$ dominates and the number of modes is independent of the dispersion. This result might be expected, since a larger dispersion not only leads to a larger beam shift, but also to beam broadening. Thus within this model of volume modes, above a certain dispersion the number of modes cannot be increased by raising the dispersion further.

Knowing how to estimate the number of modes using (6), the question is how to maximize the number of modes for a given stack. Here we will consider the case that we have designed a structure that has a certain dispersion behavior and is operated at a given incidence angle. Even though the incidence angle appears as a variable in (6), it cannot really be changed easily as the dispersion curve is only designed and valid for a certain angle. Thus, to change the input angle, we would have to design a new structure. The same argument is true for the operating range of the structure, which is also determined by the design. The only parameter we can change is the angular range of the input beam.

In (6) the thickness of the structure does not appear except that the calculation is only correct for $d<<L$ as shown in Fig. 1(a). (6) predicts more modes for a structure with a smaller input angular range. Thus, we would want to choose the input angular range as small as possible to obtain the maximum number of volume modes. But a smaller input angular range results in a larger beam waist, and the device has to have a larger thickness for the condition $d<<L$ to be true. Therefore, the only conclusion we can draw from (6) is that the angular range should be as small as possible and the thickness has to grow correspondingly. This agrees with the result given in [8] for highly dispersive photonic crystals.

3. VERIFICATION OF VOLUME MODE MODEL

In section 2. we have derived (6) for calculating the number of volume modes. In this section we will test this model by calculating the number of spatially non-overlapping volume modes for a non-periodic design with a linear change of the group propagation angle with wavelength consisting of alternating layers of SiO_2 (n=1.45) and Ta_2O_5 (n=2.09) on a quartz substrate (n=1.52) as shown in Fig. 2. Light is incident from the substrate side on the left. The multilayer stack has a total thickness of 48 μm.

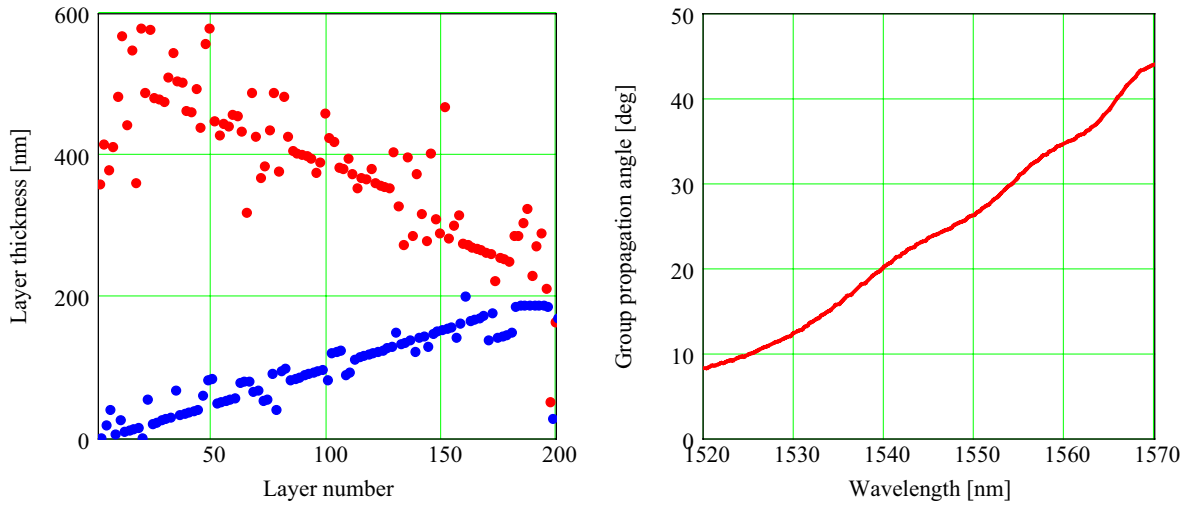

Fig. 2. Design 1 with a linear change in the group propagation angle as a function of wavelength. (a) Physical thicknesses of the SiO_2 (red) and Ta_2O_5 (blue) layers. (b) Group propagation angle at 40° incidence angle.

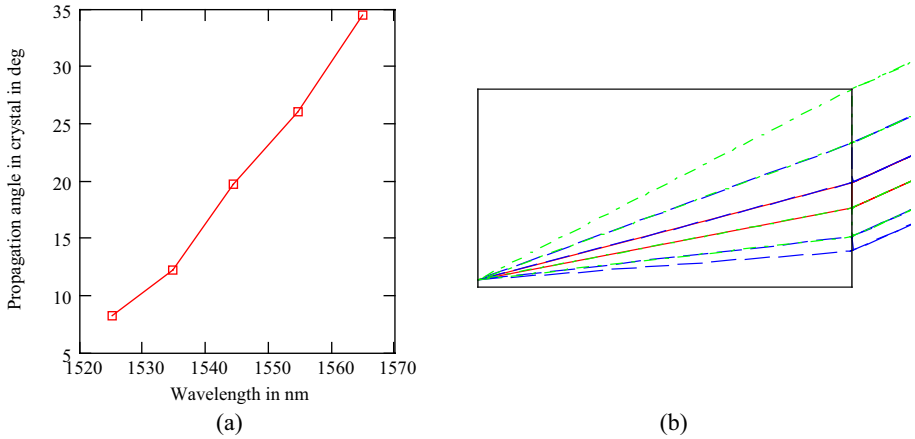

Fig. 3. Volume mode calculation for Design 1 in Fig. 2 for an incidence angle of 40°, an input half cone of 0.6°, and a wavelength interval from 1525 nm to 1565 nm. (a) shows the position of the obtained modes in terms of wavelength and low propagation angle within the crystal. (b) depicts a cartoon of the obtained modes.

Wavelength in nm	Low angle in °	High angle in °
1525	8.24	12.26
1535	12.26	19.74
1544	19.75	25.99
1554	26.00	34.50
1565	34.50	43.79

Table 1. Wavelength, low angle, and high angle of the different modes for the example in Fig. 3.

Assuming that the width d of the modes at the input surface is negligible compared to the length of the structure L ($d<<L$), the number of modes supported by the structure is numerically obtained as follows. First the angular range of the mode with the lowest wavelength is calculated from the input angular range. Fig. 3 gives an example of such a calculation. The lowest mode is chosen to have a wavelength of 1525 nm. From Table 1 we see that this mode occupies an angular range from 8.24° to 12.26°. Now we know that the next higher mode has to have at least a low angle of

12.26°. Using a numerical search algorithm, we find the next possible mode to have a wavelength of 1535 nm and an angular range in the structure of 12.26° to 19.74°. We continue to find modes in this manner until the high wavelength of 1565 nm in this example is reached. Table 1 gives the numerical data for the five modes found. In Fig. 3(b) a cartoon of the modes is depicted.

Using the numerical simulation technique described above, we can now test the theoretical number of modes expected from (6) against the number of modes actually obtained. Using (6) the number of modes for Design 1 is calculated as a function of the input angular range $\Delta\theta_{in}$. The integral is performed by calculating ten intermediate points. Only the dispersion $Disp_{\omega}$ is assumed to be a function of frequency. The resulting number of modes is plotted as the crosses in Fig. 4. The number of modes is rounded off to the previous integer, since fractional modes are physically not possible. The squares plotted in Fig. 4 represent the number of modes obtained from a numerical simulation as described above.

Fig. 4 nicely shows the agreement between simulation and theoretical number of modes obtained for the volume mode model (6). Also we see again that the number of modes is inversely proportional to the input angular range as predicted before. Thus, we would want to choose a small angular range, e.g. 0.2°, which corresponds to a spot size (Gaussian beam radius) of 140 μm. But if d is about twice the spot size, the thickness L of the stack would have to be several times this value for the condition $d<<L$ to be fulfilled.

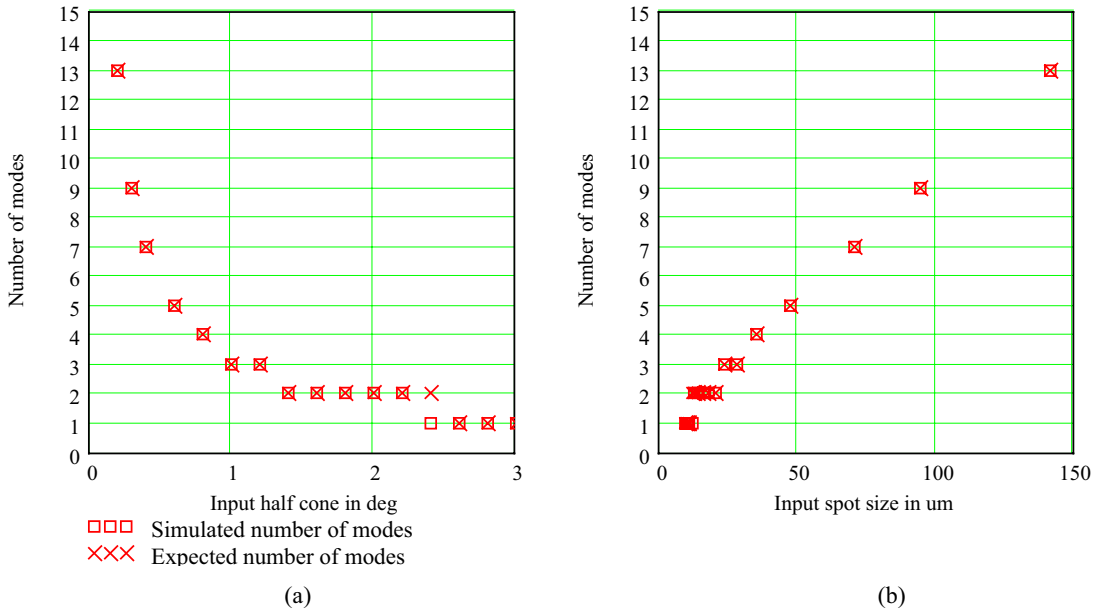

Fig. 4. Number of volume modes as obtained from simulation and the expected number of modes calculated using (6) as a function of the input half cone in (a) and the input spot size in (b).

4. NUMBER OF SURFACE MODES

For wavelength multiplexing and demultiplexing applications, separable WDM modes have to be spatially non-overlapping at the output interface, but not necessarily within the structure. This results in a mode picture as given in Fig. 1(b). Here we assume that the backside is the output surface of interest, i.e. the position where we place the detectors or output waveguides. Any other plane could be chosen equally well, as this is a linear system. A separate lens may be necessary to focus the light onto the output devices in that case. Assuming a monotonically increasing group propagation angle θ_{group} with frequency, the number of modes within a frequency range ω_1 to ω_2 is given by the total shift in this range divided by the surface Δx occupied by one mode. Furthermore, we have already one mode without any dispersion, which is added in (7).

$$N_{modes}\left(\tilde{\theta},\tilde{\omega}_1,\tilde{\omega}_2,\Delta x\right)=\frac{L\left(\tan\left(\theta_{group}\left(\tilde{\theta},\tilde{\omega}_2\right)\right)-\tan\left(\theta_{group}\left(\tilde{\theta},\tilde{\omega}_1\right)\right)\right)}{\Delta x}+1 \tag{7}$$

In order to calculate the number of modes within a frequency range $\Delta\omega$, we start from expression (8) for the number of modes within an angular range $\Delta\theta_{group}$.

$$\Delta N_{modes}\left(\tilde{\theta},\tilde{\omega},\Delta\theta_{group},\Delta x\right)=\frac{L\left(\tan\left(\theta_{group}\left(\tilde{\theta},\tilde{\omega}\right)+\frac{\Delta\theta_{group}}{2}\right)-\tan\left(\theta_{group}\left(\tilde{\theta},\tilde{\omega}\right)-\frac{\Delta\theta_{group}}{2}\right)\right)}{\Delta x} \tag{8}$$

Using identity (9), (8) can be approximated by (10).

$$\tan\alpha\pm\tan\beta=\frac{\sin\left(\alpha\pm\beta\right)}{\cos\alpha\cos\beta} \tag{9}$$

$$\Delta N_{modes}\left(\tilde{\theta},\tilde{\omega},\Delta\theta_{group},\Delta x\right)=\frac{L\,\Delta\theta_{group}}{\Delta x\cos^2\left(\theta_{group}\left(\tilde{\theta},\tilde{\omega}\right)\right)} \tag{10}$$

Finally, plugging in the definition of the dispersion $Disp_\omega$ as defined in (2), we obtain the number of modes within a frequency range $\Delta\omega$ as given in (11).

$$\Delta N_{modes}\left(\tilde{\theta},\tilde{\omega},\Delta\omega,\Delta x\right)=\frac{L\,Disp_\omega\left(\tilde{\theta},\tilde{\omega}\right)\Delta\omega}{\Delta x\cos^2\left(\theta_{group}\left(\tilde{\theta},\tilde{\omega}\right)\right)} \tag{11}$$

If Δx or $Disp_\omega$ are not the same for all the modes, but a function of frequency, (11) can be integrated to obtain the number of modes within a frequency range as given in (12).

$$N_{modes}\left(\tilde{\theta},\omega_1,\omega_2,\Delta x\right)=1+\int_{\omega_1}^{\omega_2}\frac{L\,Disp_\omega\left(\tilde{\theta},\tilde{\omega}\right)}{\Delta x\cos^2\left(\theta_{group}\left(\tilde{\theta},\tilde{\omega}\right)\right)}d\tilde{\omega} \tag{12}$$

Now we consider again the question, how to maximize the number of modes obtained for a given dispersion curve and given incidence angle. We see that we get more modes the larger the thickness L of the stack is and the smaller the surface Δx occupied by one mode is. In the volume-mode calculation, we assumed that the input beam is focused on the front surface of the structure. But this is not necessary for wavelength multiplexing devices. From (12) we see that we obtain a larger number of modes if the beam is focused on the output surface.

For a general structure, only one mode will be focused exactly at the backside of the structure occupying a surface depending on the spot size w_0. Other modes will be out of focus and require a larger area. Given a certain structure, the focus has to be chosen in such a way that the largest number of modes can be fitted on the back surface. In principle, a structure could be designed in such a way that all modes focus at the same distance L from the front surface. This will allow for the largest number of modes possible, since moving any mode out of focus will increase its size Δx and therefore lower the total number of modes.

Concluding this argument, we see from (12) that a larger thickness L of the stack and a smaller surface Δx occupied by each mode lead to a larger number of modes. Again we did not find a real optimal beam size. The number of modes is larger the smaller the beam waist is. One limit to decreasing the beam waist further is given by the fact that a smaller beam waist means a larger input angular range and thus a larger area of the dispersion curve is probed as discussed in [7]. Since the dispersion curve is only valid over a certain wavelength range and thus over a certain angular range, this limits the size of the input beam.

5. MAXIMUM NUMBER OF SURFACE MODES INCLUDING BOUNCES

In this section we will consider the maximum number of surface modes if we include multiple bounces off the stack as shown in Fig. 1(c). As discussed in the last section the highest number of modes is obtained if all modes are focused on the output surface. The condition of all modes focussing on the output surface is approximately equivalent to having a constant spatial dispersion with wavelength [10], i.e. the beam experiences a linear shift s along the output surface as a function of wavelength for operation in reflection as in Fig. 1(c). s is calculated by (13).

$$s = 2L\tan\left(\theta_{group}\right) \tag{13}$$

Therefore, the optimal structure should have a constant dispersion as defined in (14).

$$Disp_{s\lambda}\left(\tilde{\theta},\tilde{\omega}\right) = \frac{\partial s\left(\tilde{\theta},\tilde{\omega}\right)}{\partial\lambda\left(\tilde{\omega}\right)} \tag{14}$$

The simplest type of structure that has a constant dispersion $Disp_{s\lambda}$ for focussing all modes at the same position is a structure that has a linear shift as a function of wavelength. Other structures can fulfill the condition as well though. The change in the shift only has to be constant over the input angular range $\Delta\theta$ corresponding to a specific frequency range $\Delta\omega$ at the position of the different channels. It is still fulfilled if there are discontinuities between the center positions of the different channels such as in a step-design [7]. The definition of the dispersion with respect to the wavelength λ has the advantage that the dispersion is without dimension in this case and does not change upon scaling the device.

Next let us consider the maximum number of channels we obtain under the condition that all channels are focussed at the output plane and therefore have an equal spatial extent Δx and are equally spaced in wavelength. For the following calculations we will consider structures with a linear shift as a function of wavelength and thus a constant dispersion $Disp_{s\lambda} = c_{Disp}$. For operation in transmission, c_{Disp} is the dispersion in transmission, while for operation upon reflection, it is the dispersion after one bounce. Thus, to obtain the total dispersion we need to multiply by the number of bounces N_b. With these considerations the number of surface modes for the situation in Fig. 1(c) is obtained as (15).

$$N_{modes}\left(c_{Disp},\lambda_1,\lambda_2,\Delta x\right) = 1+\int_{\lambda_1}^{\lambda_2}\frac{N_b\,c_{Disp}}{\Delta x}\,d\lambda = 1+\frac{N_b\,c_{Disp}}{\Delta x}\left(\lambda_2-\lambda_1\right) \tag{15}$$

In this calculation the channel spacing $\Delta\lambda$ is given by (16).

$$\Delta\lambda = \frac{\Delta x}{N_b\,c_{Disp}} \tag{16}$$

Also, the number of modes agrees with the picture of dividing the total bandwidth by the bandwidth of one mode as given in (17).

$$N_{modes} = 1+\frac{\lambda_2-\lambda_1}{\Delta\lambda} \tag{17}$$

So far we only considered the propagation through the multilayer stack and not the propagation through the substrate. For the broadening of Gaussian beams the total propagation length is relevant. In the following it is assumed that the substrate is thick compared to the stack. Thus, the total propagation distance L_p is determined by the substrate thickness L_s and is given by (18), where θ_s is the propagation angle in the substrate.

$$L_p = \frac{2\,N_b\,L_s}{\cos\left(\theta_s\right)} \tag{18}$$

The multiplexed wavelength channels have the same spot size w_1 at the input and Δx is a constant as discussed above. While the propagation through the substrate determines the beam size, the layers only cause the beam shift and may offset the focal plane or lead to distortions. Δx is determined by crosstalk considerations. For a constant ratio $c_1=\Delta x/w_t$ the crosstalk is constant. $c_1=3.2$ corresponds to approximately -30dB crosstalk and $c_1=3.8$ to -40dB [10]. Δx is related to $\Delta\lambda$ as given in (19), where c_{Disp} is the dispersion of a single bounce and N_b is the number of bounces.

$$c_1 = \frac{\Delta x}{w_t} = \frac{\Delta\lambda\, c_{Disp}\, N_b}{w_t} \tag{19}$$

The beam propagates as a Gaussian beam within the structure. The beam broadening limits the number of bounces. In order to keep the field of the different bounces separated, (20) follows from Fig. 1(c).

$$\frac{d_1}{w_1} \geq 2 \tag{20}$$

In (20) d_1 is the separation between the center of the different bounces and w_1 is the spot size along the interface at the entering surface. d_1 is calculated with (21), where θ_s is the propagation angle in the substrate.

$$d_1 = 2L_s \tan(\theta_s) \tag{21}$$

The beam size of a Gaussian beam $w(z)$ is given by (22) and (23) [11].

$$w(z) = w_0\sqrt{1+\left(\frac{z}{z_R}\right)^2} \tag{22}$$

$$z_R = \frac{\pi\, {w_0}^2\, n}{\lambda} \tag{23}$$

Using these equations, w_1 can be approximated for a propagation distance $z>> z_R$ as in (24). The subscript "s" refers to the values within the substrate.

$$w_1 = \frac{w\left(\frac{2N_b L_s}{\cos(\theta_s)}\right)}{\cos(\theta_s)} = \frac{w_s}{\cos(\theta_s)}\sqrt{1+\left(\frac{2N_b L_s/\cos(\theta_s)}{\frac{\pi\, {w_s}^2 n_s}{\lambda}}\right)^2} \approx \frac{w_s}{\cos(\theta_s)}\frac{2N_b L_s \lambda}{\pi\, {w_s}^2 n_s \cos(\theta_s)} \tag{24}$$

Substituting (21) and (24) into (20) we obtain (25).

$$\frac{2L_s\tan(\theta_s)}{\frac{w_s}{\cos(\theta_s)}\frac{2N_b L_s\lambda}{\pi\, {w_s}^2 n_s\cos(\theta_s)}} = \frac{\sin(\theta_s)\cos(\theta_s)^2\pi\, w_t\, n_s}{N_b\lambda} \geq 2 \tag{25}$$

Thus, condition (26) needs to be fulfilled for non-overlapping bounces.

$$w_t \geq \frac{2N_b\lambda}{\sin(\theta_s)\cos(\theta_s)^2\pi\, n_s} \tag{26}$$

(26) is a very important equation, since it defines how far we can reduce the spot size. In section 4 we saw that we get more modes the smaller we choose the spot size. Now we have a condition for the smallest spot size. Thus, the maximum

number of modes is obtained if the equal sign in (26) is fulfilled. Substituting (26) into (19), we get condition (27) for $\Delta\lambda$.

$$\Delta\lambda = \frac{c_1 w_t}{c_{Disp} N_b} \geq \frac{2c_1 \lambda}{c_{Disp} \sin(\theta_s)\cos(\theta_s)^2 \pi n_s} \tag{27}$$

Finally, using (17) we obtain the maximum number of surface modes possible on the wavelength interval from λ_1 to λ_2 as shown in (28).

$$N_m = 1 + \frac{\lambda_2 - \lambda_1}{\Delta\lambda} \leq 1 + \frac{(\lambda_2 - \lambda_1) c_{Disp} \sin(\theta_s)\cos(\theta_s)^2 \pi n_s}{2c_1 \lambda} \tag{28}$$

Or, rewriting (28) in terms of the incident angle in air, we reach (29) for the maximum number of surface modes including multiple bounces.

$$N_m \leq 1 + \frac{(\lambda_2 - \lambda_1)}{\lambda} \frac{\pi c_{Disp} \sin(\theta)\left(1 - \frac{\sin(\theta)^2}{n_s{}^2}\right)}{2c_1} \quad \text{for } z >> z_R \tag{29}$$

(29) assumes that the channels are focussed at the output surface. In principle we could perform double the number of bounces such that the channels are focussed after half the bounces and the exit beam size is identical to the incident beam size. In this case we obtain twice as many channels, but we need to use a second lens on the output side to refocus the channels.

It is interesting to note in (29) that increasing the number of bounces or decreasing the spot size cannot increase the number of surface modes. For a given crosstalk, the beam size determines the number of bounces to be performed. The first factor in expression (29) shows that only the relative wavelength interval matters. All designs are scalable to a different wavelength range and have, after the scaling, the same number of modes as before. As expected, either a higher dispersion or a larger crosstalk (smaller c_1) leads to a larger number of modes. Furthermore, a larger index of refraction in the substrate also increases the number of modes. The number of modes is approximately independent of the angle, if the incident angle is larger than 40°.

6. VERIFICATION OF SURFACE MODE MODEL

Similarly to the verification of the volume mode model in section 3 we will here test the surface mode model by numerical simulation of the number of surface modes for Design 1 in Fig. 2. The number of surface modes can be calculated numerically by determining the number of non-overlapping channels along the exit surface of the structure. First we determine, which wavelength is going to be focused at the exit interface in distance L. In the example of Fig. 5 the center wavelength 1545 nm of the interval is chosen to be focused with a spot size of 20μm. Now we calculate how large the spot size w_1 at the input interface has to be for that beam to be focused. Together with the incidence angle and the focal spot size, this completely determines the Gaussian beam at the input interface.

The first mode is chosen to be at the lowest wavelength, here at 1525 nm. For this mode the 1/e-E-field rays are calculated and the cross points with the exit interface are determined. Table 2 lists the calculated angles for the two 1/e-E-field rays and the position where they cross the back interface. If a mode is focused on the backside, the rays cross at that position and the spot size along the interface is $w_t = w_0/\cos(\theta)$ resulting in a separation between modes given by $\Delta x = c_{1*} w_t$. For a mode that is not focused on the backside, a larger surface area Δx is needed. Here the surface area is increased by the amount between the two rays. This is not exactly right, but a sufficiently good approximation.

The second mode can now be calculated by searching numerically for a mode that is separated by the spacing width $c_{1*} w_t$ from the first mode. In our example the next mode is found to have a wavelength of 1542 nm. Table 2 lists the

numerical data for the five modes obtained. From the table we see that the modes overlap in angle, but are spatially separated at the output surface. The distance between the high point of one mode and the low point of the next mode is always separated by the spacing of 100 µm. In Fig. 5(b) the modes are shown graphically. Even though the structure is operated in reflection and with multiple bounces, the beam path is unfolded in the forward direction. As different wavelengths propagate in parallel in the substrate, the substrate changes the focal position approximately equally for all beams. Thus, it does not need to be considered. It is clearly visible that the three center modes in Fig. 5(b) are quite well focused while the outer modes are running out of focus.

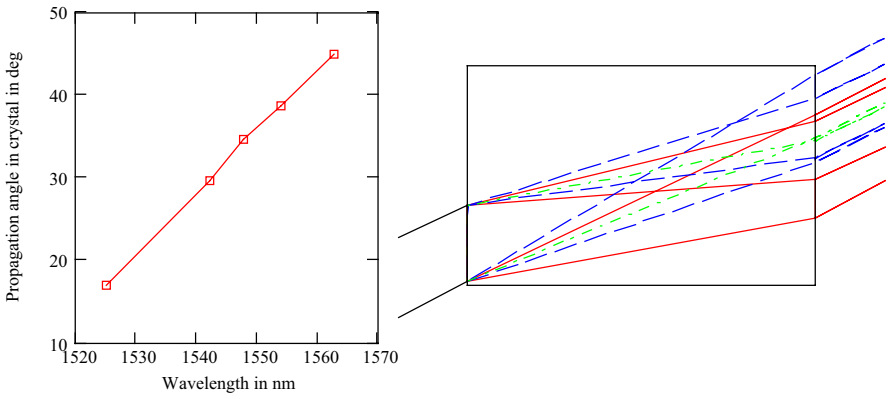

(a) (b)

Fig. 5. Surface mode calculation for Design 1 in Fig. 2 for an incidence angle of 40°, focussing on the back side at 1545 nm with a spot size of 20 µm (corresponding to $\Delta\theta_{in}$ = 1.4°), a wavelength interval from 1525 nm to 1565 nm, and 13 bounces. To obtain a crosstalk around –40dB, a spacing of 3.8*20 µm/cos(40°)=100 µm is chosen between modes. (a) shows the position of the obtained modes in terms of wavelength and propagation angle within the crystal. (b) depicts a cartoon of the modes obtained graphing the two 1/e E-field rays for each mode.

Wavelength in nm	Angle$^+$ in °	Angle$^-$ in °	Position$^+$ in µm	Position$^-$ in µm
1525	16.96	6.81	382.3	610.4
1542	29.58	12.95	711.6	748.7
1548	34.59	17.26	864.5	849.9
1554	38.70	21.95	1004.0	965.7
1563	44.91	27.23	1250.0	1106.0

Table 2. Wavelength, group propagation angle in the structure for the input angle plus the half cone angle (Angle$^+$), group propagation angle minus the half cone angle (Angle$^-$), position where the plus-angle crosses the back interface (Position$^+$), and position where the minus-angle crosses the back interface (Position$^-$) for the different modes for the example in Fig. 5.

Now we can compare the number of modes predicted by (12) against the number of modes obtained by simulation. For the calculation of the integral in (12) ten intermediate points are used and a sum is formed. Since the input angular range $\Delta\theta_{in}$ =1.4° is rather large, the difference is not replaced by a differential to determine the angular range within the structure $\Delta\theta_{struc}$. The maximum number of surface modes for a given dispersion is calculated using (29), where Δx is assumed to be the constant $\Delta x = c_{1*} w_t$ independent of wavelength.

Fig. 6 graphs the expected number of modes from (12), the maximum number of modes from (29), and the simulated number of modes as a function of the number of bounces. The expected number of modes agrees well with the simulated number of modes verifying (12) for modeling the number of surface modes. The number of modes obtained with this design remains significantly below the maximum number of modes though. This is due to the fact that not all the modes are focused. Some of the surface space is used for unfocused modes instead of for new modes as visible in Fig. 5(b). In order to obtain the maximum number of modes, all the modes have to be focused on the backside, i.e. the beam exit position should change linearly as a function of wavelength. Such a design is introduced in the next section.

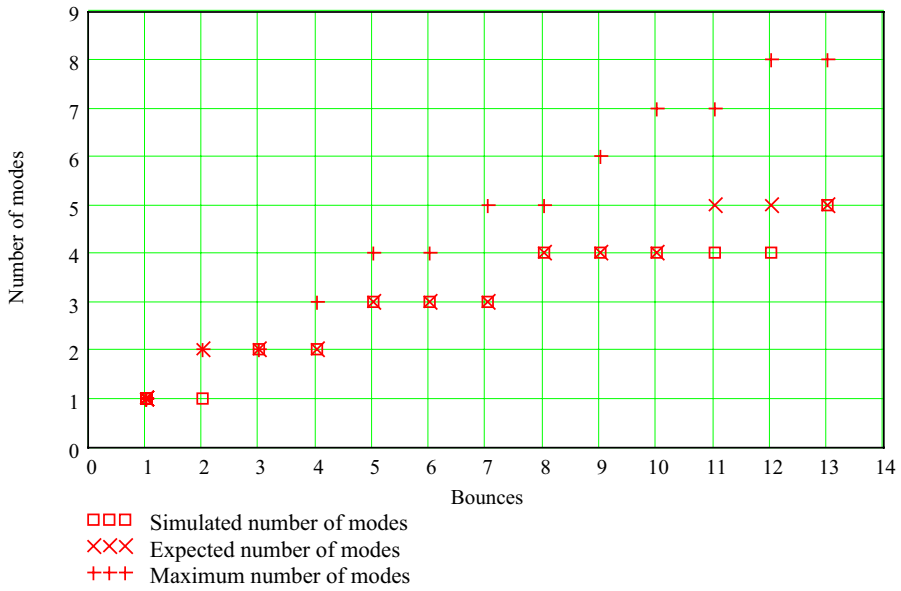

Fig. 6. Number of surface modes as obtained from simulation, the expected number of modes calculated using (12), and the maximum number of modes obtained from (29) for Design 1 as a function of the number of bounces within the structure.

7. DESIGNING FOR A MAXIMUM NUMBER OF MODES

In the preceding sections we concluded that the surface mode picture is valid to calculate the number of Gaussian modes supported by a structure for WDM applications. The total number of modes is limited by the condition that the field of consecutive bounces should not overlap and is given by (29). To obtain the maximum number of modes, the shift of the structure has to be linear with wavelength. In this case all modes can be focused on the exit surface of the structure. An example structure with a linear shift was designed. Design 2 has again 200 layers and a thickness of 49 µm. Fig. 7 shows the physical thickness of the layers as a function of the layer position within the stack. The shift of this design is nicely linear with a dispersion of c_{Disp} = 1.4 µm/nm.

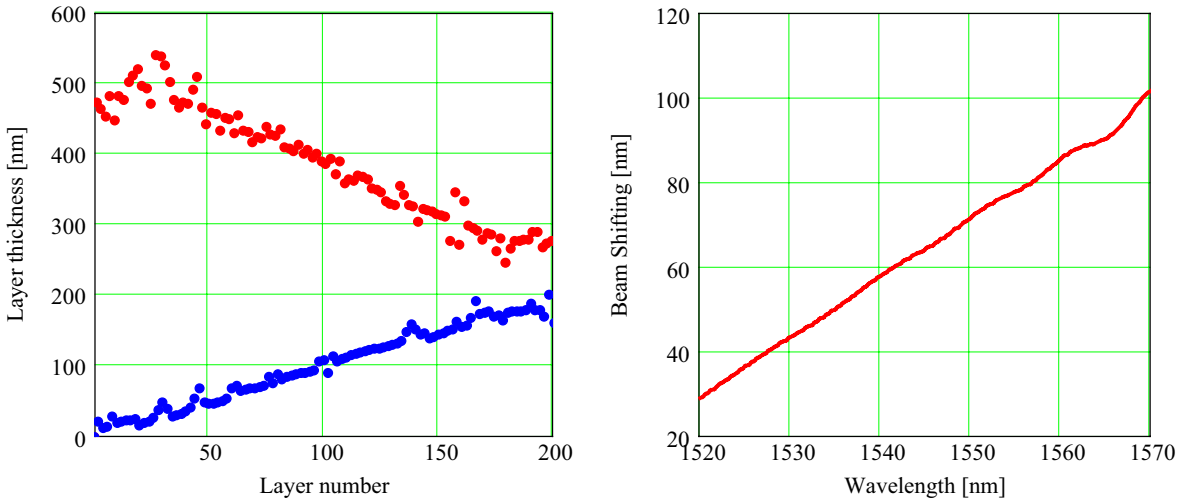

Fig. 7. Design 2 with a linear spatial beam shifting as a function of wavelength. (a) Physical thicknesses of the SiO_2 (red) and Ta_2O_5 (blue) layers. (b) Spatial beam shifting at 40° incidence angle.

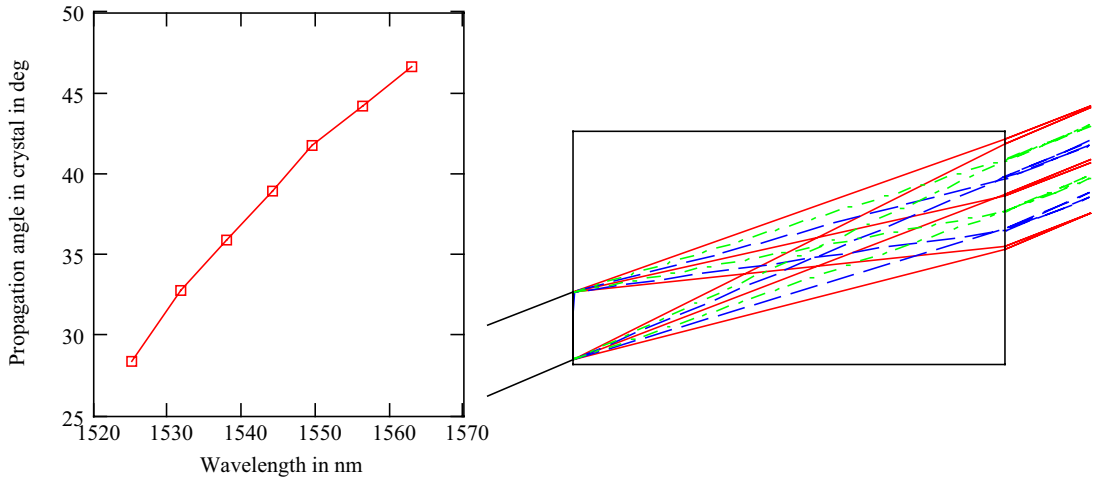

Fig. 8. Surface mode calculation for Design 2 for an incidence angle of 40°, focussing on the back side at 1545 nm with a spot size of 20 µm (corresponding to $\Delta\theta_{in}$ = 1.4°), a wavelength interval from 1525 nm to 1565 nm, and 13 bounces. To obtain a crosstalk around –40dB, a spacing of 3.8*20 µm/cos(40°)=100 µm is chosen between modes. (a) shows the position of the modes obtained, in terms of wavelength and propagation angle within the crystal. (b) depicts a cartoon of the obtained modes graphing the two 1/e-E-field rays for each mode.

Wavelength in nm	Angle$^+$ in °	Angle$^-$ in °	Position$^+$ in µm	Position$^-$ in µm
1525	28.33	12.58	684.9	708.0
1532	32.69	16.85	815.3	809.2
1538	35.81	21.30	916.5	919.7
1544	38.91	25.15	1025.0	1021.0
1549	41.69	28.92	1132.0	1126.0
1556	44.14	32.88	1233.0	1246.0
1563	46.68	36.80	1347.0	1375.0

Table 3. Wavelength, group propagation angle in the structure for the input angle plus the half cone angle (Angle$^+$), group propagation angle minus the half cone angle (Angle$^-$), position where the plus-angle crosses the back interface (Position$^+$), and position where the minus-angle crosses the back interface (Position$^-$) for the different modes for the example in Fig. 8.

Using (29) the maximum number of modes possible with this design in the wavelength interval from 1525 nm to 1565 nm is obtained to be N_m=8. For a spot size of 20 µm at the focus, this requires 13.7 bounces within the structure. Since only an integer number of bounces can be performed, we will use 13 bounces. Fig. 8 shows the result of the numerical simulation of this structure and Table 3 gives the data corresponding to the modes. The cartoon in Fig. 8(b) depicts that all modes are focused on the back interface of the structure. Instead of the theoretical limit of eight modes, seven modes are obtained with this structure. This is due to the reduction of the number of bounces from 13.7 to 13.

In Fig. 9 the simulated, the expected, and the maximum number of modes are given as a function of the number of bounces within the structure. It can be seen that for 13 bounces only seven modes are predicted. The quality of the design can also be seen in the fact that the expected and the maximum number of modes are nearly identical. Furthermore, the number of modes obtained in the simulation also agrees with the maximum number of modes. Thus, we accomplished our goal of designing a structure that supports the maximum number of modes for the given dispersion.

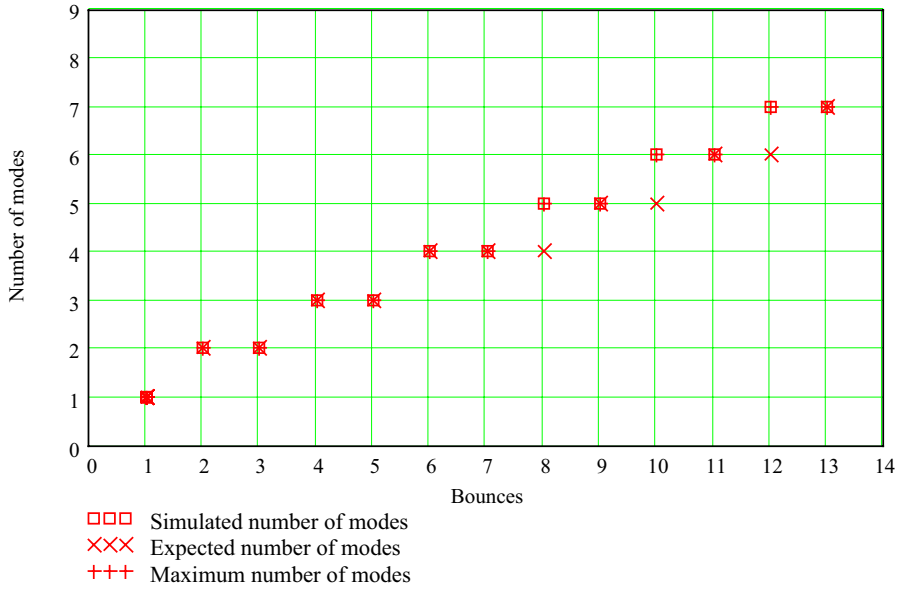

Fig. 9. Number of surface modes as obtained from simulation, the expected number of modes calculated using (12), and the maximum number of modes obtained from (29) for Design 2 as a function of the number of bounces within the structure.

8. CONCLUSIONS

We developed two different models for calculating the possible number of channels for a given structure. The volume mode model is based on the assumption that different wavelength channels should propagate in mutually exclusive propagation cones within the volume of the dispersive structure. It is shown that the number of volume modes is independent of the dispersion (except if the dispersion is low) and proportional to the diameter of the input beam. Therefore the maximum possible beam diameter should be chosen to obtain the maximum number of separable volume channels. On the other hand, the structure has to be larger than the beam diameter resulting in the necessity of large structures.

For some applications it might be desirable to separate the different wavelength channels within the volume of the dispersive structure. For wavelength multiplexing and demultiplexing devices though it is sufficient to separate the different WDM channels on the output surface. This is equivalent to the situation in an arrayed waveguide grating (AWG), where the different wavelength channels are separated at the plane of the output waveguides but not throughout the entire AWG structure. We developed a model for estimating the number of WDM channels that can be separated along the output surface of a dispersive photonic nanostructure. We show that the number of separable channels is proportional to the dispersion and to the wavelength range over which this dispersion is achieved normalized by the center wavelength. Therefore, scaling a design to a different wavelength does not change the number of achievable modes. The number of modes is reduced for more stringent crosstalk requirements. Including multiple bounces the number of modes is independent of the beam diameter, since the number of bounces is limited by beam broadening.

It is important to stress that a high dispersion value alone does not guarantee a high number of separable WDM channels, but that the product of dispersion and wavelength range over which this dispersion is achieved should be maximized. Therefore, the total spatial shift achieved with a photonic nanostructure is a better figure of merit than the dispersion. One-dimensional photonic crystals have, e.g., regions of very high dispersion close to the stop band edge, but since this dispersion is only achieved over a very narrow wavelength range, these structures are not useful as WDM devices.

The separable number of WDM channels is calculated for two 200-layer non-periodic thin-film stacks and verified by numerical simulation. It is shown that a structure with a linear beam shifting as a function of wavelength is

advantageous, since all wavelength channels have the same focal plane and the maximum number of channels is achieved. Using the 200-layer stack eight WDM channels may be multiplexed or demultiplexed making this a promising device for coarse wavelength division multiplexing (CWDM) applications.

ACKNOWLEDGMENTS

This work was supported by the DARPA Optocenters Program. M. Gerken acknowledges support of the Sequoia Capital Stanford Graduate Fellowship.

REFERENCES

[1] R. Zengerle, "Light propagation in singly and doubly periodic planar waveguides," J. Mod. Opt., **34**/12 (1987), 1589-1617.

[2] B. E. Nelson, M. Gerken, D. A. B. Miller, R. Piestun, C.-C. Lin, J. S. Harris, Jr., "Use of a dielectric stack as a one-dimensional photonic crystal for wavelength demultiplexing by beam shifting," Opt. Lett. **25**/20 (2000), 1502-1504.

[3] L. Wu, M. Mazilu, T. Karle, T. F. Krauss, "Superprism Phenomena in Planar Photonic Crystals," IEEE J. Quantum Electron., **38**/7 (2002), 915-918.

[4] H. Kosaka, T. Kawashima, A. Tomita, M. Notomi, T. Tamamura, T. Sato, S. Kawakami, "Superprism phenomena in photonic crystals," Phys. Rev. B, **58**/16 (1998), R10 096-R10 099.

[5] M. Gerken and D. A. B. Miller, "Multilayer thin-film structures with high spatial dispersion," *Appl. Opt.*, **42**/7, 1330-1345 (2003).

[6] M. Gerken and D. A. B. Miller, "Wavelength Demultiplexer Using the Spatial Dispersion of Multilayer Thin-Film Structures," *IEEE Photonics Techn. Lett.* **15**/8, 1097-1099 (2003).

[7] M. Gerken and D. A. B. Miller, "Multilayer Thin-Film Stacks With Steplike Spatial Beam Shifting," *J. Lightwave Techn.*, **22**/2, 612-618 (2004).

[8] T. Baba and T. Matsumoto, "Resolution of photonic crystal superprism," *Appl. Phys. Lett.*, **81**/13 (2002), 2325-2327.

[9] D. A. B. Miller, "Communicating with waves between volumes - evaluating orthogonal spatial channels and limits on coupling strengths," Appl. Opt. **39**, 1681 – 1699 (2000).

[10] M. Gerken, *Wavelength Multiplexing by Spatial Beam Shifting in Multilayer Thin-Film Structures*, Electrical Engineering Ph.D. Dissertation, Stanford University, March 2003.

[11] A. E. Siegman, *Lasers*, University Science Books, Sausalito, CA (1986).